

1. Introduction

Volumetric capture stages provide a compelling platform for recording human performances in 3D, enabling applications such as immersive telepresence, virtual production, and mixed-reality content creation. These systems allow for captured performances to be replayed from arbitrary viewpoints and inserted into novel environments. Realizing this potential, however, requires addressing two fundamental challenges: *novel view synthesis*, to render unseen perspectives from sparse camera inputs, and *relighting*, to adapt the captured content to new lighting conditions so that it blends naturally into target scenes.

The first challenge, novel view synthesis (NVS), has witnessed extraordinary progress in recent years. Breakthroughs such as Neural Radiance Fields (NeRF) [52] and 3D Gaussian Splatting [36], together with a large body of follow-up work [17], have demonstrated the ability to generate photorealistic renderings from sparse views with remarkable fidelity. By combining multi-view cues with expressive scene representations that capture geometry and appearance, these approaches have transitioned from academic prototypes to production-ready tools, establishing a new foundation for volumetric video pipelines [1, 69].

The second challenge, relighting, has been extensively studied, but remains difficult in capture stages where inputs are sparse, lighting is uniform, and material or illumination cues are limited. While one-light-at-a-time (OLAT) capture can enable high-quality relighting [66, 73], it remains impractical for most applications. Inverse rendering provides a principled formulation, yet becomes ill-posed under limited observations needed for dynamic acquisition. Recent data-driven approaches, including diffusion-based decomposition models, offer a promising alternative by directly predicting material and illumination properties from images [34, 43, 58, 81].

This motivates our central question: *Are diffusion relighting models ready for capture stage compositing?* While their progress is promising, it remains unclear whether these models can meet the demands of real-world use when integrated into volumetric capture pipelines. In this work, we revisit the relighting problem from a practical perspective with an emphasis on stability. We propose a simple yet effective approach that leverages priors from state-of-the-art decomposition models while avoiding the complexity and instability of full inverse rendering or generative diffusion methods. To this end, we introduce a flow-guided temporal regularization scheme for consistent material estimates and a lightweight screen-space relighting module inspired by real-time graphics pipelines with efficient shadow computation. By combining learned priors with physically informed design choices, our method achieves more stable and accurate relighting, making it better suited for production pipelines in volumetric capture.

Contributions. In summary, our contributions are

- An end-to-end relighting pipeline for volumetric capture, where we present a practical, production-ready relighting framework that integrates state-of-the-art image decomposition priors with physically-motivated rendering, enabling consistent and photorealistic results across dynamic sequences.
- Temporal regularization for dynamic relighting that mitigates flickering and appearance instability, preserving both fine details and smooth lighting transitions over time.
- Comprehensive evaluation of the usability of diffusion-based relighting approaches for in real-world volumetric capture scenarios, highlighting trade-offs in quality, stability, and computational cost.

2. Related Work

Material Estimation and Relighting Material estimation and relighting aim to recover surface reflectance properties and scene illumination, enabling realistic appearance synthesis under novel lighting conditions. Classical approaches formulate this task as an inverse rendering problem; owing to its inherent ill-posedness, early methods rely on strong, hand-crafted priors [4, 5, 10, 84]. A closely related direction focuses on estimating material appearance parameterized as a spatially varying BRDF (SVBRDF), again leveraging carefully designed priors [2, 49]. The advent of deep learning has relaxed many of these constraints, enabling SVBRDF estimation from a single texture image [18, 67] or from multi-view observations [19]. More recently, deep learning-based inverse rendering frameworks have coupled differentiable rendering with neural networks to jointly recover geometry, reflectance, and illumination from single-view [39, 40, 61, 72, 76], dual-view [7], or multi-view inputs [16, 46].

Recent years have seen significant progress in neural methods for relighting, which aim to synthesize novel illuminations for existing scenes or objects. Neural Radiance Fields (NeRF) [52] have been extended to support relighting by explicitly modeling material and illumination properties, via intrinsic decomposition of scene properties [8, 60, 64, 83], or via a learned scene representation using One-Light-at-a-Time (OLAT) recordings [73]. The introduction of 3D Gaussian Splatting (3DGS) [36] has led to diverse relighting strategies, via intrinsic decomposition [22, 28, 44, 45, 62], or relighting using OLAT data [6, 20, 48]. Some neural relighting methods avoid 3D reconstruction altogether, operating entirely in image space, e.g. by modelling view- and light-dependent transport as a learned function [82] or training a CNN [74] to predict relit results from sparse lighting samples.

More recently, diffusion models with their strong generative expression have been applied to relighting problems. Among these, Ren *et al.* proposed an image hormiza-

tion, where they focus on light adaptation based on the background [58], followed by IC-Light [81] addressing illumination harmonization via text prompt guided background generation. Various works discuss relighting via text prompts [34, 38, 80] or light controlled image generation [79]. Neural Gaffer [34] propose relighting by either text prompt or environment map. While these approaches provide good results for single view images, the state-of-the-art Diffusion Renderer [43] unifies inverse and forward rendering within a video diffusion framework. This approach can reduce temporal inconsistencies – which are inherent in single-image settings, since diffusion models tend to produce different outputs for even slightly different inputs – but its applicability is limited by the large memory requirements. These constraints make it less suitable for high-resolution, multi-view capture stages, where consistency across views is essential. We discuss potential strategies to make its use feasible in such scenarios.

Novel-View Synthesis Novel-view synthesis aims to generate images of a scene from viewpoints not present in the input observations. Early approaches for novel view synthesis primarily relied on rendering from images, and depth-guided warping techniques [12, 13, 23, 31]. Learning-based methods have since been proposed for novel view synthesis using multiplane images [25, 41, 51, 63] or voxel embeddings [33, 50]. More recently, neural radiance fields became the prevalent approach for novel view synthesis [52]. Since then, many variants focusing on more efficient scene representation have been proposed, such as low-rank factorized 4D grid scene representation [14], sparse 3D voxel grids with spherical harmonics [26], additional non-linearity in grid values [35], and directly optimized dense voxel grids [65]. Beyond static scene acceleration, research has expanded NeRFs to dynamic environments [27, 42, 55–57], enabling relighting by scene decomposition [8, 9, 64, 83]; improving the rendering of glossy surfaces via alternative radiance parameterizations [68], developing face-specific relighting methods [60], while others proposed scene editing without re-training [78]. Real-time rendering has likewise become a key focus [29, 53, 75], and recent work has moved toward alternative representations such as 3D Gaussian Splatting [36], which replaces implicit fields with explicit point-based primitives for real-time rendering. Subsequent work has further improved both rendering speed [3, 24, 30, 32, 54] and quality [47, 70, 71]. Additional advances have extended Gaussian-based methods beyond basic rendering, such as incorporating subsurface scattering [21] and enabling real-time relighting of head avatars [59]. In parallel, researchers have explored Gaussian-based surface reconstruction techniques [15, 77], further broadening their applicability to geometry recovery tasks.

3. Hybrid Relighting Framework

Our method combines three key components as shown in Fig. 2: volumetric scene representations for novel view synthesis and proxy geometry (Sec. 3.1), estimation and regularization of intrinsic material properties (Sec. 3.2 and Sec. 3.3) and a physically based relighting stage that produces view-consistent shading under novel illumination (Sec. 3.4). The final compositing step accounts for indirect interactions such as cast shadows and reflections, ensuring that the subject integrates plausibly with its surroundings. In the following, we describe each of these stages in detail.

3.1. Novel View Synthesis & Indirect Interactions

Given a multi-camera capture of a performance, our goal is to render the subject from novel viewpoints and to integrate it into a new environment with plausible *indirect interactions*, specifically cast shadows on nearby receivers and reflection contributions, while supporting *relighting*. To achieve this, we ideally need a NVS representation that provides (i) RGB appearance, (ii) depth maps, (iii) surface normals, and (iv) a proxy geometry suitable for integration into conventional rendering engines. Gaussian Opacity Fields (GOF) [77] are a natural choice, as they jointly optimize for appearance and normals, produce accurate depth estimates, and allow mesh extraction for downstream use.

However, we observe that GOF reconstructions often suffer from artifacts: curved, natural surfaces are approximated as piecewise planar surfaces, and spurious holes may appear. To mitigate these issues, we introduce two additional regularization terms during optimization: a Huber-regularized total variation loss on the rendered depth map, and an edge-aware Laplacian smoothness prior on the Gaussian normal map. Let $z(x, y)$ denote the rendered depth map. We enforce spatial smoothness with a Huber loss-based total variation penalty:

$$\mathcal{L}_{\text{depth}} = \sum_{x,y} H_{\delta}\left(\frac{\partial z}{\partial x}\right) + H_{\delta}\left(\frac{\partial z}{\partial y}\right) \quad (1)$$

where H_{δ} denotes Huber loss (cf. Eq. (6)). To prevent blocky surface approximations while respecting appearance discontinuities, we penalize the Laplacian of the estimated normal field $n(x, y)$ in an edge-aware fashion with respect to the RGB image $I(x, y)$ as

$$\mathcal{L}_{\text{normal}} = \sum_{x,y} \exp\left(-\frac{\|\nabla I(x,y)\|^2}{2\sigma^2}\right) \cdot \|\Delta n(x,y)\|^2, \quad (2)$$

where σ is a contrast sensitivity parameter. Intuitively, smoothing is encouraged in homogeneous regions while being suppressed at edges aligned with appearance boundaries.

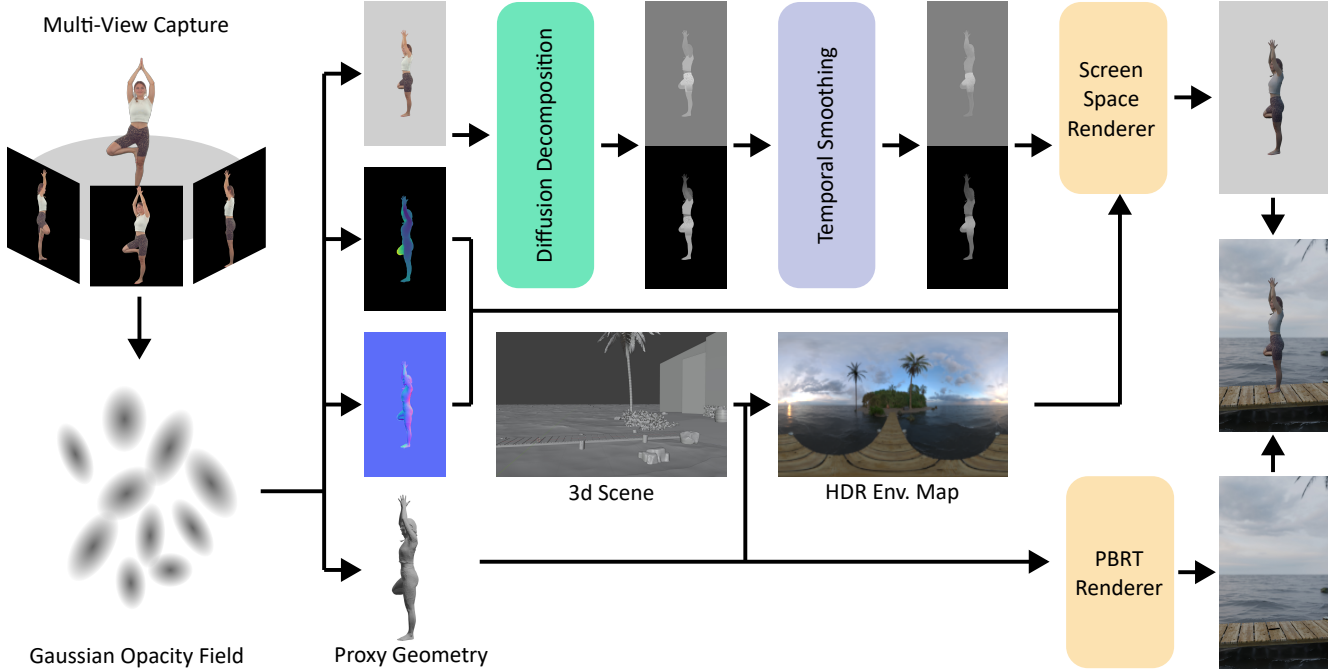


Figure 2. We optimize a Gaussian Opacity Field [77] from multi-view captures to render RGB, depth and normal maps for the novel views and extract a proxy mesh (left). Using a diffusion decomposition model [43] we extract roughness and metallic maps, which we smooth using an optical-flow guided temporal regularization (top). We render the proxy geometry as a shadow caster in the 3d scene (bottom) and blend it with out screen space rendered image (right).

Proxy Mesh for Indirect Interactions. The extracted GOF mesh enables conventional rendering of indirect effects in external engines such as Blender. By inserting the mesh into the background scene and disabling intersections with foreground camera rays, we obtain plausible cast shadows and reflection contributions without requiring perfect geometry or material accuracy. Since indirect effects are typically low-frequency, coarse geometry suffices for the majority of capture scenarios to render plausible background images.

3.2. Hybrid G-Buffer Estimation

We estimate G-buffer channels using learned predictions for view- and light-independent material properties. We consider the problem of predicting roughness r and metallic μ maps, from a single color image $I \in \mathbb{R}^{H \times W \times 3}$ by employing the intrinsic decomposition model \mathcal{D}_θ from [43] that provides the mapping

$$\mathcal{D}_\theta : I \rightarrow \{r, \mu\}. \quad (3)$$

Since diffusion sampling is stochastic, we draw K samples per input in order to estimate both mean predictions and per-pixel uncertainty. To allow high-resolution processing, inference is carried out on overlapping patches $I^{(j)}$ as

$$\hat{x}^{(i,j)} = \mathcal{D}_\theta(I^{(j)}; \xi_i), \quad i = 1, \dots, K \quad (4)$$

where ξ_i denotes the diffusion noise. These patchwise predictions are then blended into full-resolution maps $\tilde{x}^{(i)}$, yielding an ensemble $\{\tilde{x}^{(1)}, \dots, \tilde{x}^{(K)}\}$ from which we compute per-pixel means and variances, thereby suppressing sampling variability and exposing an uncertainty signal useful for downstream processing.

3.3. Temporal Consistency via Optical Flow-Guided Regularization

We next enforce consistency across neighboring renderings. Let $\tilde{x} \in \{\tilde{r}, \tilde{\mu}\}$ denote the per-pixel mean prediction and σ_x the corresponding normalized standard deviation. Let $m_\alpha = \mathbb{1}_{\alpha > 0.5}$ be a binary foreground mask, and let \mathcal{W} denote backward warping from frame $t+1$ to t using estimated optical flow. We write \odot for element-wise multiplication and \mathcal{V} to denote a binary map of valid flows which point to valid foreground $\mathcal{W}(m_\alpha)$ and are forward/backward consistent. The temporally regularized estimate x_t at step t is obtained by minimizing

$$\arg \min_x \sum_t \langle H_\delta(\tilde{x}_t - x_t), 1 - \sigma_{x,t} \rangle + \lambda_1 TV_\varepsilon(x_t) + \lambda_2 \|(\mathcal{W}(x_t) - x_t) \odot \mathcal{V}\|_2^2 \quad (5)$$

where $\langle \cdot, \cdot \rangle$ is the element-wise inner product and H_δ is the (element-wise) Huber loss

$$H_\delta(a) = \begin{cases} \frac{1}{2}a^2 & \text{if } |a| < \delta \\ \delta(|a| - \frac{1}{2}\delta) & \text{otherwise.} \end{cases} \quad (6)$$

The (smoothed) isotropic total variation is

$$\text{TV}_\varepsilon(x^t) = \sum_i \sqrt{\|\nabla_x x_i^t\|_2^2 + \|\nabla_y x_i^t\|_2^2} + \varepsilon, \quad (7)$$

for small ε . The first term in Eq. (5) is a confidence-weighted data fidelity loss that aligns x with the diffusion prediction \tilde{x} , with deviations weighted according to prediction confidence (i.e., lower weight in regions of high uncertainty). The second term enforces spatial smoothness through total variation regularization, and the third term constrains temporal consistency by penalizing discrepancies between the current roughness or metallic estimate and its backward-warped counterpart.

3.4. Relighting and Compositing

We perform single-image environment relighting using albedo, depth, normals, roughness and metallic estimated as described above. Shading is computed using Disney’s Principled BRDF [11] using a Cook–Torrance microfacet BRDF with a GGX normal distribution, Smith geometry term, and Schlick Fresnel approximation. Illumination is provided by a high-dynamic-range environment map rendered from the target scene at the approximate actor location. For each environment direction, we evaluate the BRDF contribution modulated by a soft shadow term, which is computed by ray-marching from each surface point along the light direction in view space. At each step, the sample position is projected back into screen space, and the depth buffer is queried to detect occluders. An occlusion factor is accumulated over all steps, then normalized to produce a soft shadow map in the range $[0, 1]$.

We composite the gamma-corrected, relit foreground with the target background using the alpha channel from the GOF render.

4. Experiments

We analyze the performance of diffusion-based methods for relighting across multiple scenes and lighting conditions, and demonstrate that our approach offers advantages in terms of robustness and visual reliability. Our evaluation comprises qualitative results on both real volumetric recordings and synthetic data (Sec. 4.1), complemented by a quantitative analysis on the synthetic dataset (Sec. 4.2). To further demonstrate the effectiveness of individual components of our method, we include an ablation study (Sec. 4.3), and discuss limitations in Sec. 4.4.

For comparison, we benchmark our approach against several recent state-of-the-art methods in neural relighting and rendering, including NVIDIA Diffusion Renderer [43], Neural Gaffer [34], IC-Light [81], Gaussian Opacity Fields (GOF) [77], and Relightable 3D Gaussian (R3DG) [28].

Datasets Our real-world evaluation is based on an extended set of various scenes from the RIFTCast dataset [85]. Each scene consists of 36 high-resolution color images at a resolution of 24.5 MP, captured within a calibrated light stage with cameras arranged in a cylindrical rig of 5.25 meters in diameter. We constructed 12 diverse target environments in Blender to place the captured content.

For a controlled analysis of the relighting, we additionally constructed a synthetic dataset of 10 rendered objects in a virtual light stage imitating the above setup. The target images are illuminated under 11 HDR environment maps at 1920×1080 resolution from 4 viewpoints, covering diverse geometry and material properties that span both diffuse and specular reflectance.

Implementation Details All experiments are implemented in PyTorch. We use the Adam optimizer [37] with its default parameters.

4.1. Qualitative Evaluation

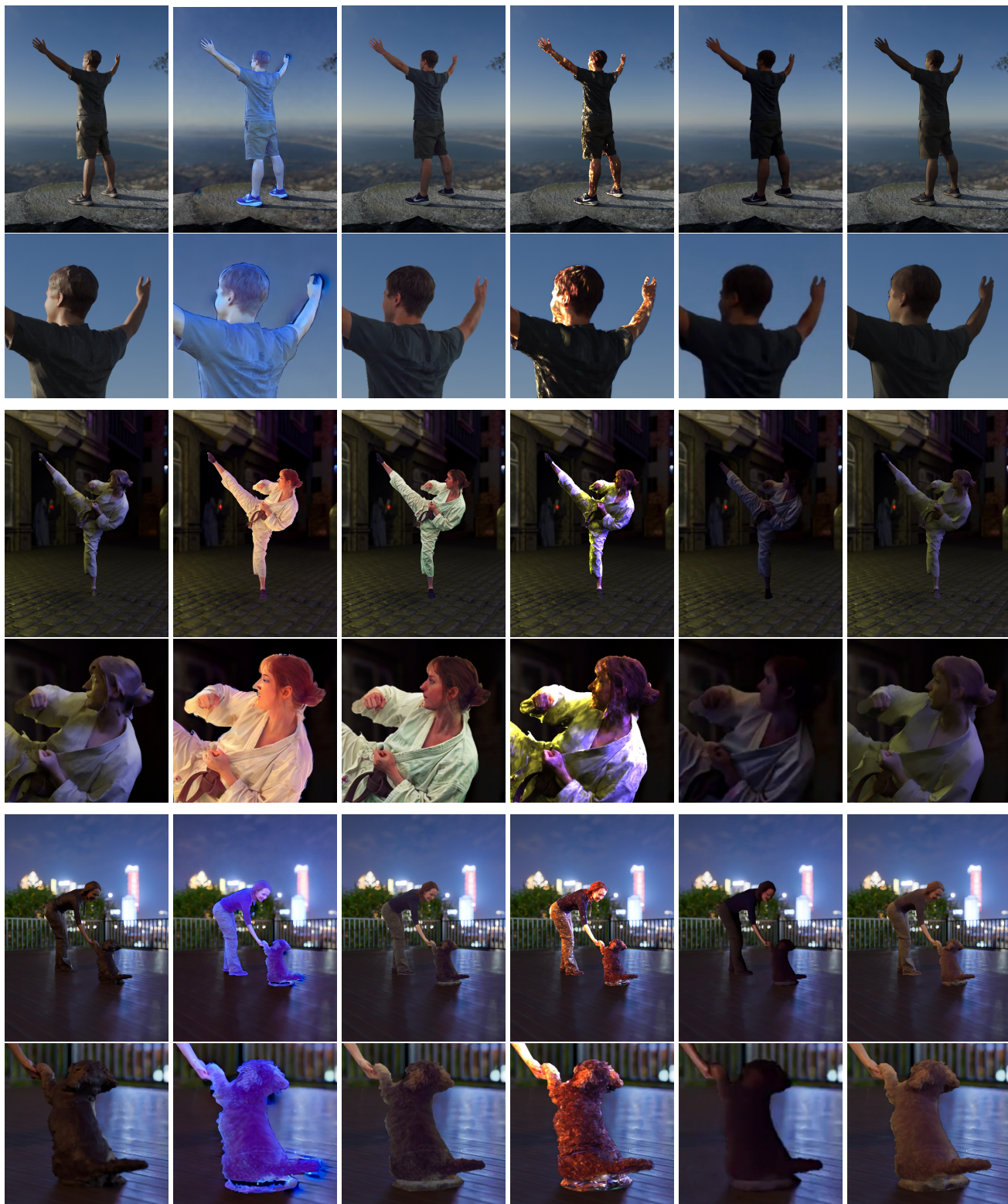
In Fig. 3, we compare our method against recent state-of-the-art diffusion-, and Gaussian-based relighting approaches. Across diverse scenes and lighting conditions, our results achieve sharper details and more realistic, spatially consistent relighting. Note that the Diffusion Renderer was evaluated at a reduced resolution of 896×512 , since its full-resolution outputs at 1920×1080 showed severe artifacts and degraded visual quality.

To further highlight the improvements over GOF, we provide an additional comparison in Fig. 4, focusing on challenging regions such as hair. Our method recovers clean alpha values instead of relying on coarse mesh representations, resulting in more natural boundaries. We also observe smoother surface reconstruction, which is particularly noticeable in the arm region, where GOF often produces sharp edges.

Finally, we also report qualitative results on the synthetic dataset in Fig. 5. These examples show ground-truth renderings alongside our relit outputs.

4.2. Numerical Analysis of Relighting Accuracy

We complement our qualitative evaluation with a quantitative analysis on object relighting on the synthetic dataset. To this end, we render ground-truth references under a wide range of environment maps and measure reconstruction accuracy across competing methods. Table 1 summarizes the results across standard image-based metrics.



GOF Mesh [77] IC-Light [81] Neural Gaffer [34] R3DG [28] Diff. Renderer [43] Yesnt (Ours)

Figure 3. Qualitative comparison with recent state-of-the-art relighting methods. Each row corresponds to a different scene under novel lighting conditions. Top panels show the full relit view, while bottom panels provide close-up crops.

Table 1. Quantitative comparison of relighting accuracy on synthetic data for diffusion-based methods. GOF is included for reference.

Method	Conditioning	PSNR \uparrow	SSIM \uparrow	LPIPS \downarrow
GOF Mesh [77]	HDR Env. Map	29.4181 ± 5.7897	0.9458 ± 0.0397	0.0619 ± 0.0552
IC-Light [81]	LDR Background	19.4115 ± 4.5775	0.9078 ± 0.0810	0.0873 ± 0.0839
Neural Gaffer [34]	HDR+LDR Env. Map	24.4263 ± 4.5009	0.9166 ± 0.0837	0.0836 ± 0.0918
Diffusion Renderer [43]	LDR+Log Env. Map	27.4926 ± 6.1947	0.9374 ± 0.0501	0.0817 ± 0.0710
Yesnt (Ours)	HDR Env. Map	30.1918 ± 5.4833	0.9580 ± 0.0284	0.0523 ± 0.0462

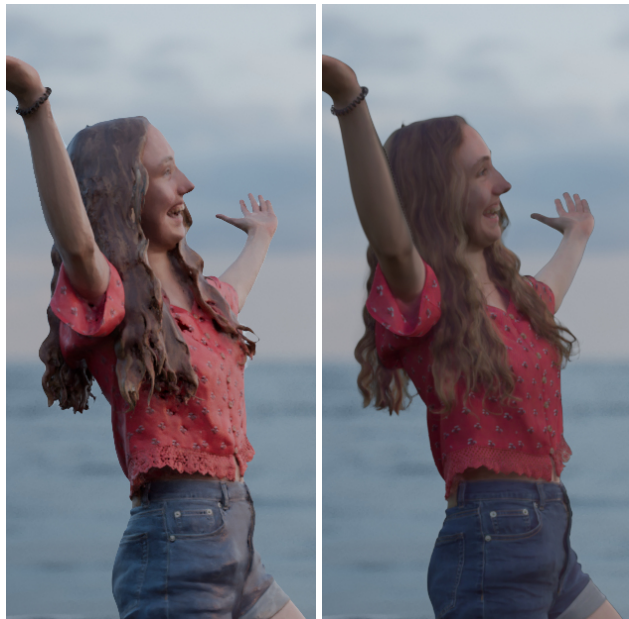


Figure 4. Comparison of relighting quality between GOF meshes [77] (left) and our method (right). GOF often approximates natural regions such as the arm with piecewise planar surfaces, whereas our approach produces smoother reconstructions and cleaner alpha mattes in challenging areas like hair.

Our method consistently achieves the best scores across all three metrics. In particular, it improves PSNR by a clear margin over all competing diffusion-based approaches, while also yielding the highest SSIM and lowest LPIPS. GOF serves as a strong geometric baseline, yet it is limited by hard surface boundaries and struggles in regions with complex transparency, as already seen qualitatively. In contrast, our pipeline maintains both high fidelity and perceptual quality across diverse lighting conditions.

4.3. Ablation Study

We conduct an ablation study to assess the contribution of individual components of our model. Tab. 2 reports results when removing either the relighting branch or the estimation of G-Buffer maps (roughness/metallic). Without relighting, the network reduces to a pure NVS model and

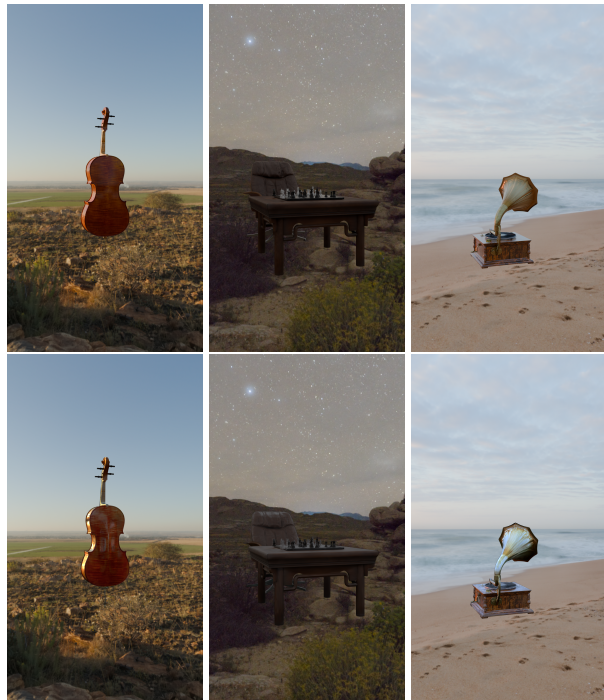


Figure 5. Qualitative results on the synthetic dataset, showing ground truth (top) and our method (bottom).

achieves substantially lower accuracy. Removing the intrinsic decomposition and keeping roughness and metallic constant also results in a notable drop across all metrics, showing that physically meaningful intermediate representations are crucial for high-fidelity relighting. The full model achieves the highest scores across all metrics.

We further evaluate the effect of temporal regularization, as introduced in Sec. 3.3. Tab. 3 compares the full model against a variant without temporal regularization. The latter suffers from degraded temporal PSNR (tPSNR) and a higher perceptual path length (PPL), indicating the presence of flickering artifacts across video frames. Note, that while PPL is typically defined in the context of latent interpolations in generative models, we compute it directly across consecutive output frames to measure frame-to-frame perceptual variation. Fig. 6 illustrates this flick-

Table 2. Ablation study of our model, comparing variants without any relighting (*i.e.* novel view synthesis only), without estimation of G-Buffer maps (roughness and metallic), and the full model.

Variant	PSNR \uparrow	SSIM \uparrow	LPIPS \downarrow
No Relighting	22.8414	0.9265	0.0742
No Decomposition	28.5688	0.9507	0.0565
Full	30.1918	0.9580	0.0523

Table 3. Temporal regularization ablation on videos (see Sec. 3.3). Removing temporal regularization (w/o Temporal Reg.) leads to a decrease in temporal PSNR (tPSNR) and larger PPL, indicating stronger flickering artifacts.

Variant	tPSNR \uparrow	PPL \downarrow
w/o Temporal Reg.	28.8737	0.3598
Full	29.3660	0.3587

Table 4. Runtimes Analysis of our method compared to others. Bottlenecks are the Gaussian model optimization and the diffusion evaluations.

Step	Runtime
<i>Per Scene</i>	
GOF – Optimization [77]	1.1 h
R3DG – Optimization [28]	0.9 h
<i>Per Frame</i>	
GOF – Rendering	0.4 s
Diffusion Decomposition	80 s
Temporal Regularisation	1.5 s
Relighting	1.5 s
Full Pipeline	87 s
IC-Light [81]	14 s
Neural Gaffer [34]	18 s
R3DG – Relighting [28]	1 s
Diffusion Renderer [43]	28 s

ering effect on predicted roughness maps: the Diffusion Renderer [43] exhibits strong temporal inconsistency across consecutive frames, whereas our flow-guided smoothing produces temporally coherent results while preserving spatial detail. These findings underline the importance of temporal regularization for stable relighting in dynamic scenes.

4.4. Limitations

In terms of efficiency, the runtime of our method is dominated by the diffusion decomposition stage (cf. Tab. 4). Our method assumes a single environment-map illumination and does not model spatially varying light sources, which limits

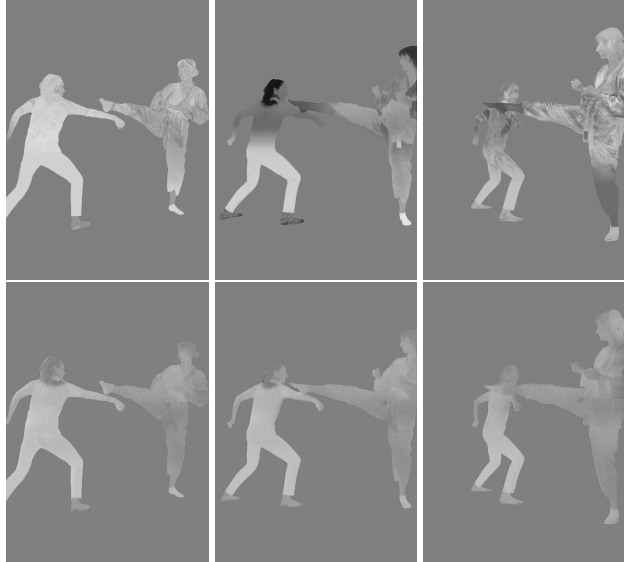


Figure 6. Top: Roughness maps predicted by the Diffusion Renderer [43] across three consecutive frames, showing strong temporal inconsistency. Bottom: Our flow-guided smoothing produces temporally coherent roughness estimates while preserving spatial detail.

local light transport effects (e.g., missing cast shadows on limbs). Finally, our approach relies on diffusion predictions being approximately correct on average. When the model yields inconsistent hypotheses across frames, the temporal regularizer suppresses these variations, leading to over-smoothing and a loss of fine detail and contrast.

5. Conclusion

We asked: *Are diffusion relighting models ready for capture stage compositing?* While they produce impressive results, they do not scale well to longer sequences. By aggregating stochastic material estimates and enforcing temporal coherence with flow-guided smoothing, our method addresses this shortcoming. Experiments on real and synthetic captures show higher fidelity and reduced flicker, bridging the gap between prototypes and production pipelines. In short, the answer is *Yesnt*: diffusion models alone are not yet ready, but our hybrid approach offers a practical path toward production-ready volumetric video relighting.

Acknowledgments

This work has been funded by the Ministry of Culture and Science North Rhine-Westphalia under grant number PB22-063A (InVirtuo 4.0: Experimental Research in Virtual Environments). We are deeply grateful to Janelle Pfeifer for her invaluable assistance during data capture and processing.

References

- [1] Arcturus studio: Experience sports like never before. Online; commercial volumetric video / immersive sports capture and experiences, 2025. Website of Arcturus Studio, describing event capture, volumetric video, and immersive replay pipelines. 2
- [2] Miika Aittala, Tim Weyrich, and Jaakko Lehtinen. Practical svbrdf capture in the frequency domain. *ACM Trans. Graph.*, 32(4):110–1, 2013. 2
- [3] Muhammad Salman Ali, Sung-Ho Bae, and Enzo Tartaglione. Elmgs: Enhancing memory and computation scalability through compression for 3d gaussian splatting. In *2025 IEEE/CVF Winter Conference on Applications of Computer Vision (WACV)*, pages 2591–2600. IEEE, 2025. 3
- [4] Jonathan T Barron and Jitendra Malik. Shape, illumination, and reflectance from shading. *IEEE transactions on pattern analysis and machine intelligence*, 37(8):1670–1687, 2014. 2
- [5] Harry Barrow, J Tenenbaum, A Hanson, and E Riseman. Recovering intrinsic scene characteristics. *Comput. vis. syst.*, 2(3-26):2, 1978. 2
- [6] Zoubin Bi, Yixin Zeng, Chong Zeng, Fan Pei, Xiang Feng, Kun Zhou, and Hongzhi Wu. Gs3: Efficient relighting with triple gaussian splatting. In *SIGGRAPH Asia 2024 Conference Papers*, pages 1–12, 2024. 2
- [7] Mark Boss, Varun Jampani, Kihwan Kim, Hendrik Lensch, and Jan Kautz. Two-shot spatially-varying brdf and shape estimation. In *Proceedings of the IEEE/CVF Conference on Computer Vision and Pattern Recognition*, pages 3982–3991, 2020. 2
- [8] Mark Boss, Raphael Braun, Varun Jampani, Jonathan T Barron, Ce Liu, and Hendrik Lensch. Nerd: Neural reflectance decomposition from image collections. In *Proceedings of the IEEE/CVF International Conference on Computer Vision*, pages 12684–12694, 2021. 2, 3
- [9] Mark Boss, Varun Jampani, Raphael Braun, Ce Liu, Jonathan Barron, and Hendrik Lensch. Neural-pil: Neural pre-integrated lighting for reflectance decomposition. *Advances in Neural Information Processing Systems*, 34: 10691–10704, 2021. 3
- [10] Adrien Bousseau, Sylvain Paris, and Frédo Durand. User-assisted intrinsic images. In *ACM SIGGRAPH Asia 2009 papers*, pages 1–10. 2009. 2
- [11] Brent Burley and Walt Disney Animation Studios. Physically-based shading at disney. In *Acm siggraph*, pages 1–7. vol. 2012, 2012. 5
- [12] Gaurav Chaurasia, Olga Sorkine, and George Drettakis. Silhouette-aware warping for image-based rendering. In *Computer Graphics Forum*, pages 1223–1232. Wiley Online Library, 2011. 3
- [13] Gaurav Chaurasia, Sylvain Duchêne, Olga Sorkine-Hornung, and George Drettakis. Depth synthesis and local warps for plausible image-based navigation. *ACM Transactions on Graphics*, 32(3):30:1–30:12, 2013. 3
- [14] Anpei Chen, Zexiang Xu, Andreas Geiger, Jingyi Yu, and Hao Su. Tensorf: Tensorial radiance fields. In *European conference on computer vision*, pages 333–350. Springer, 2022. 3
- [15] Danpeng Chen, Hai Li, Weicai Ye, Yifan Wang, Weijian Xie, Shangjin Zhai, Nan Wang, Haomin Liu, Hujun Bao, and Guofeng Zhang. Pgsr: Planar-based gaussian splatting for efficient and high-fidelity surface reconstruction. *IEEE Transactions on Visualization and Computer Graphics*, 31(9):6100–6111, 2025. 3
- [16] JunYong Choi, SeokYeong Lee, Haesol Park, Seung-Won Jung, Ig-Jae Kim, and Junghyun Cho. Mair: multi-view attention inverse rendering with 3d spatially-varying lighting estimation. In *2023 IEEE/CVF Conference on Computer Vision and Pattern Recognition (CVPR)*, pages 8392–8401. IEEE, 2023. 2
- [17] Anurag Dalal, Daniel Hagen, Kjell G Robbersmyr, and Kristian Muri Knausgård. Gaussian splatting: 3d reconstruction and novel view synthesis: A review. *IEEE Access*, 12: 96797–96820, 2024. 2
- [18] Valentin Deschaintre, Miika Aittala, Fredo Durand, George Drettakis, and Adrien Bousseau. Single-image svbrdf capture with a rendering-aware deep network. *ACM Transactions on Graphics (ToG)*, 37(4):1–15, 2018. 2
- [19] Valentin Deschaintre, Miika Aittala, Frédo Durand, George Drettakis, and Adrien Bousseau. Flexible svbrdf capture with a multi-image deep network. In *Computer graphics forum*, pages 1–13. Wiley Online Library, 2019. 2
- [20] Jan-Niklas Dihlmann, Arjun Majumdar, Andreas Engelhardt, Raphael Braun, and Hendrik Lensch. Subsurface scattering for gaussian splatting. *Advances in Neural Information Processing Systems*, 37:121765–121789, 2024. 2
- [21] Jan-Niklas Dihlmann, Arjun Majumdar, Andreas Engelhardt, Raphael Braun, and Hendrik P.A. Lensch. Subsurface scattering for gaussian splatting. In *Advances in Neural Information Processing Systems*, pages 121765–121789. Curran Associates, Inc., 2024. 3
- [22] Kang Du, Zhihao Liang, and Zeyu Wang. Gs-id: Illumination decomposition on gaussian splatting via diffusion prior and parametric light source optimization. *arXiv preprint arXiv:2408.08524*, 2024. 2
- [23] Martin Eisemann, Bert De Decker, Marcus Magnor, Philippe Bekaert, Edilson De Aguiar, Naveed Ahmed, Christian Theobalt, and Anita Sellent. Floating textures. In *Computer graphics forum*, pages 409–418. Wiley Online Library, 2008. 3
- [24] Zhiwen Fan, Kevin Wang, Kairun Wen, Zehao Zhu, Dejia Xu, Zhangyang Wang, et al. Lightgaussian: Unbounded 3d gaussian compression with 15x reduction and 200+ fps. *Advances in neural information processing systems*, 37: 140138–140158, 2024. 3
- [25] John Flynn, Michael Broxton, Paul Debevec, Matthew DuVall, Graham Fyffe, Ryan Overbeck, Noah Snively, and Richard Tucker. Deepview: View synthesis with learned gradient descent. In *Proceedings of the IEEE/CVF Conference on Computer Vision and Pattern Recognition*, pages 2367–2376, 2019. 3
- [26] Sara Fridovich-Keil, Alex Yu, Matthew Tancik, Qinhong Chen, Benjamin Recht, and Angjoo Kanazawa. Plenoxels:

- Radiance fields without neural networks. In *Proceedings of the IEEE/CVF conference on computer vision and pattern recognition*, pages 5501–5510, 2022. 3
- [27] Sara Fridovich-Keil, Giacomo Meanti, Frederik Rahbæk Warburg, Benjamin Recht, and Angjoo Kanazawa. K-planes: Explicit radiance fields in space, time, and appearance. In *Proceedings of the IEEE/CVF Conference on Computer Vision and Pattern Recognition*, pages 12479–12488, 2023. 3
- [28] Jian Gao, Chun Gu, Youtian Lin, Zhihao Li, Hao Zhu, Xun Cao, Li Zhang, and Yao Yao. Relightable 3d gaussians: Realistic point cloud relighting with brdf decomposition and ray tracing. In *European Conference on Computer Vision*, pages 73–89. Springer, 2024. 2, 5, 6, 8
- [29] Stephan J Garbin, Marek Kowalski, Matthew Johnson, Jamie Shotton, and Julien Valentin. Fastnerf: High-fidelity neural rendering at 200fps. In *Proceedings of the IEEE/CVF international conference on computer vision*, pages 14346–14355, 2021. 3
- [30] Sharath Girish, Kamal Gupta, and Abhinav Shrivastava. Eagles: Efficient accelerated 3d gaussians with lightweight encodings. In *European Conference on Computer Vision*, pages 54–71. Springer, 2024. 3
- [31] Michael Goesele, Jens Ackermann, Simon Fuhrmann, Carsten Haubold, Ronny Klowsky, Drew Steedly, and Richard Szeliski. Ambient point clouds for view interpolation. In *ACM SIGGRAPH 2010 papers*, pages 1–6. 2010. 3
- [32] Alex Hanson, Allen Tu, Geng Lin, Vasu Singla, Matthias Zwicker, and Tom Goldstein. Speedy-splat: Fast 3d gaussian splatting with sparse pixels and sparse primitives. In *Proceedings of the Computer Vision and Pattern Recognition Conference*, pages 21537–21546, 2025. 3
- [33] Tong He, John Collomosse, Hailin Jin, and Stefano Soatto. Deepvoxels++: Enhancing the fidelity of novel view synthesis from 3d voxel embeddings. In *Proceedings of the Asian conference on computer vision*, 2020. 3
- [34] Haian Jin, Yuan Li, Fujun Luan, Yuanbo Xiangli, Sai Bi, Kai Zhang, Zexiang Xu, Jin Sun, and Noah Snavely. Neural gaffer: Relighting any object via diffusion. *Advances in Neural Information Processing Systems*, 37:141129–141152, 2024. 2, 3, 5, 6, 7, 8
- [35] Animesh Karnawar, Tobias Ritschel, Oliver Wang, and Niloy Mitra. Relu fields: The little non-linearity that could. In *ACM SIGGRAPH 2022 conference proceedings*, pages 1–9, 2022. 3
- [36] Bernhard Kerbl, Georgios Kopanas, Thomas Leimkühler, and George Drettakis. 3d gaussian splatting for real-time radiance field rendering. *ACM Trans. Graph.*, 42(4):139–1, 2023. 2, 3
- [37] Diederik P Kingma. Adam: A method for stochastic optimization. *arXiv preprint arXiv:1412.6980*, 2014. 5
- [38] Peter Kocsis, Julien Philip, Kalyan Sunkavalli, Matthias Nießner, and Yannick Hold-Geoffroy. Lightit: Illumination modeling and control for diffusion models. In *Proceedings of the IEEE/CVF Conference on Computer Vision and Pattern Recognition*, pages 9359–9369, 2024. 3
- [39] Zhengqi Li and Noah Snavely. Cgintrinsics: Better intrinsic image decomposition through physically-based rendering. *Proceedings of the European conference on computer vision (ECCV)*, pages 371–387, 2018. 2
- [40] Zhengqi Li, Mohammad Shafiei, Ravi Ramamoorthi, Kalyan Sunkavalli, and Manmohan Chandraker. Inverse rendering for complex indoor scenes: Shape, spatially-varying lighting and svbrdf from a single image. In *Proceedings of the IEEE/CVF conference on computer vision and pattern recognition*, pages 2475–2484, 2020. 2
- [41] Zhengqi Li, Wenqi Xian, Abe Davis, and Noah Snavely. Crowdsampling the plenoptic function. In *European Conference on Computer Vision*, pages 178–196. Springer, 2020. 3
- [42] Zhengqi Li, Simon Niklaus, Noah Snavely, and Oliver Wang. Neural scene flow fields for space-time view synthesis of dynamic scenes. In *Proceedings of the IEEE/CVF conference on computer vision and pattern recognition*, pages 6498–6508, 2021. 3
- [43] Ruofan Liang, Zan Gojcic, Huan Ling, Jacob Munkberg, Jon Hasselgren, Chih-Hao Lin, Jun Gao, Alexander Keller, Nandita Vijaykumar, Sanja Fidler, et al. Diffusion renderer: Neural inverse and forward rendering with video diffusion models. In *Proceedings of the Computer Vision and Pattern Recognition Conference*, pages 26069–26080, 2025. 2, 3, 4, 5, 6, 7, 8
- [44] Zhihao Liang, Hongdong Li, Kui Jia, Kailing Guo, and Qi Zhang. Gus-ir: Gaussian splatting with unified shading for inverse rendering. *arXiv preprint arXiv:2411.07478*, 2024. 2
- [45] Zhihao Liang, Qi Zhang, Ying Feng, Ying Shan, and Kui Jia. Gs-ir: 3d gaussian splatting for inverse rendering. In *Proceedings of the IEEE/CVF Conference on Computer Vision and Pattern Recognition*, pages 21644–21653, 2024. 2
- [46] Yehonathan Litman, Or Patashnik, Kangle Deng, Aviral Agrawal, Rushikesh Zawar, Fernando De la Torre, and Shubham Tulsiani. Materialfusion: Enhancing inverse rendering with material diffusion priors. *arXiv preprint arXiv:2409.15273*, 2024. 2
- [47] Rong Liu, Rui Xu, Yue Hu, Meida Chen, and Andrew Feng. Atoms: Atomizing gaussian splatting for high-fidelity radiance field. *arXiv preprint arXiv:2405.12369*, 2024. 3
- [48] Zhenyuan Liu, Yu Guo, Xinyuan Li, Bernd Bickel, and Ran Zhang. Bigs: Bidirectional gaussian primitives for relightable 3d gaussian splatting. *arXiv preprint arXiv:2408.13370*, 2024. 2
- [49] Stephen Lombardi and Ko Nishino. Single image multimaterial estimation. In *2012 IEEE Conference on Computer Vision and Pattern Recognition*, pages 238–245. IEEE, 2012. 2
- [50] Stephen Lombardi, Tomas Simon, Jason Saragih, Gabriel Schwartz, Andreas Lehrmann, and Yaser Sheikh. Neural volumes: Learning dynamic renderable volumes from images. *arXiv preprint arXiv:1906.07751*, 2019. 3
- [51] Ben Mildenhall, Pratul P Srinivasan, Rodrigo Ortiz-Cayon, Nima Khademi Kalantari, Ravi Ramamoorthi, Ren Ng, and Abhishek Kar. Local light field fusion: Practical view synthesis with prescriptive sampling guidelines. *ACM Transactions on Graphics (ToG)*, 38(4):1–14, 2019. 3

- [52] Ben Mildenhall, Pratul P Srinivasan, Matthew Tancik, Jonathan T Barron, Ravi Ramamoorthi, and Ren Ng. Nerf: Representing scenes as neural radiance fields for view synthesis. *Communications of the ACM*, 65(1):99–106, 2021. 2, 3
- [53] Thomas Müller, Alex Evans, Christoph Schied, and Alexander Keller. Instant neural graphics primitives with a multiresolution hash encoding. *ACM transactions on graphics (TOG)*, 41(4):1–15, 2022. 3
- [54] Michael Niemeyer, Fabian Manhardt, Marie-Julie Rakotosaona, Michael Oechsle, Daniel Duckworth, Rama Gosula, Keisuke Tateno, John Bates, Dominik Kaeser, and Federico Tombari. Radsplat: Radiance field-informed gaussian splatting for robust real-time rendering with 900+ fps. *arXiv preprint arXiv:2403.13806*, 2024. 3
- [55] Keunhong Park, Utkarsh Sinha, Jonathan T Barron, Sofien Bouaziz, Dan B Goldman, Steven M Seitz, and Ricardo Martin-Brualla. Nerfies: Deformable neural radiance fields. In *Proceedings of the IEEE/CVF international conference on computer vision*, pages 5865–5874, 2021. 3
- [56] Keunhong Park, Utkarsh Sinha, Peter Hedman, Jonathan T Barron, Sofien Bouaziz, Dan B Goldman, Ricardo Martin-Brualla, and Steven M Seitz. Hypernerf: A higher-dimensional representation for topologically varying neural radiance fields. *arXiv preprint arXiv:2106.13228*, 2021.
- [57] Albert Pumarola, Enric Corona, Gerard Pons-Moll, and Francesc Moreno-Noguer. D-nerf: Neural radiance fields for dynamic scenes. In *Proceedings of the IEEE/CVF conference on computer vision and pattern recognition*, pages 10318–10327, 2021. 3
- [58] Mengwei Ren, Wei Xiong, Jae Shin Yoon, Zhixin Shu, Jianming Zhang, HyunJoon Jung, Guido Gerig, and He Zhang. Relightful harmonization: Lighting-aware portrait background replacement. In *Proceedings of the IEEE/CVF Conference on Computer Vision and Pattern Recognition*, pages 6452–6462, 2024. 2, 3
- [59] Shunsuke Saito, Gabriel Schwartz, Tomas Simon, Junxuan Li, and Giljoo Nam. Relightable gaussian codec avatars. In *Proceedings of the IEEE/CVF Conference on Computer Vision and Pattern Recognition (CVPR)*, pages 130–141, 2024. 3
- [60] Kripasindhu Sarkar, Marcel C Bühler, Gengyan Li, Daoye Wang, Delio Vicini, Jérémy Riviere, Yinda Zhang, Sergio Orts-Escolano, Paulo Gotardo, Thabo Beeler, et al. Litnerf: Intrinsic radiance decomposition for high-quality view synthesis and relighting of faces. In *SIGGRAPH Asia 2023 Conference Papers*, pages 1–11, 2023. 2, 3
- [61] Soumyadip Sengupta, Jinwei Gu, Kihwan Kim, Guilin Liu, David W Jacobs, and Jan Kautz. Neural inverse rendering of an indoor scene from a single image. In *Proceedings of the IEEE/CVF International Conference on Computer Vision*, pages 8598–8607, 2019. 2
- [62] Yahao Shi, Yanmin Wu, Chenming Wu, Xing Liu, Chen Zhao, Haocheng Feng, Jian Zhang, Bin Zhou, Errui Ding, and Jingdong Wang. Gir: 3d gaussian inverse rendering for relightable scene factorization. *IEEE Transactions on Pattern Analysis and Machine Intelligence*, 2025. 2
- [63] Pratul P Srinivasan, Richard Tucker, Jonathan T Barron, Ravi Ramamoorthi, Ren Ng, and Noah Snavely. Pushing the boundaries of view extrapolation with multiplane images. In *Proceedings of the IEEE/CVF Conference on Computer Vision and Pattern Recognition*, pages 175–184, 2019. 3
- [64] Pratul P Srinivasan, Boyang Deng, Xiuming Zhang, Matthew Tancik, Ben Mildenhall, and Jonathan T Barron. Nerv: Neural reflectance and visibility fields for relighting and view synthesis. In *Proceedings of the IEEE/CVF conference on computer vision and pattern recognition*, pages 7495–7504, 2021. 2, 3
- [65] Cheng Sun, Min Sun, and Hwann-Tzong Chen. Direct voxel grid optimization: Super-fast convergence for radiance fields reconstruction. In *Proceedings of the IEEE/CVF conference on computer vision and pattern recognition*, pages 5459–5469, 2022. 3
- [66] Timo Teufel, Pulkit Gera, Xilong Zhou, Umar Iqbal, Pramod Rao, Jan Kautz, Vladislav Golyanik, and Christian Theobalt. Humanolat: A large-scale dataset for full-body human relighting and novel-view synthesis. In *International Conference on Computer Vision (ICCV)*, 2025. 2
- [67] Giuseppe Vecchio, Simone Palazzo, and Concetto Spampinato. Surfacerfnet: Adversarial svbrdf estimation from a single image. In *Proceedings of the IEEE/CVF international conference on computer vision*, pages 12840–12848, 2021. 2
- [68] Dor Verbin, Peter Hedman, Ben Mildenhall, Todd Zickler, Jonathan T Barron, and Pratul P Srinivasan. Ref-nerf: Structured view-dependent appearance for neural radiance fields. In *2022 IEEE/CVF Conference on Computer Vision and Pattern Recognition (CVPR)*, pages 5481–5490. IEEE, 2022. 3
- [69] VP Land. Volinga ai advances 3d gaussian splatting with professional-grade tools for film production, 2025. Industry report on Volinga Suite and Unreal plugin enabling 3DGS in professional production pipelines (ACES, HDR, integration). 2
- [70] Yiwen Wang, Siyuan Chen, and Ran Yi. Sg-splatting: Accelerating 3d gaussian splatting with spherical gaussians. *arXiv preprint arXiv:2501.00342*, 2024. 3
- [71] Haato Watanabe, Kenji Tojo, and Nobuyuki Umetani. 3d gabor splatting: Reconstruction of high-frequency surface texture using gabor noise, 2025. 3
- [72] Felix Wimbauer, Shangzhe Wu, and Christian Rupprecht. De-rendering 3d objects in the wild. In *Proceedings of the IEEE/CVF Conference on Computer Vision and Pattern Recognition*, pages 18490–18499, 2022. 2
- [73] Yingyan Xu, Gaspard Zoss, Prashanth Chandran, Markus Gross, Derek Bradley, and Paulo Gotardo. Renerf: Relightable neural radiance fields with nearfield lighting. In *Proceedings of the IEEE/CVF International Conference on Computer Vision (ICCV)*, pages 22581–22591, 2023. 2
- [74] Zexiang Xu, Kalyan Sunkavalli, Sunil Hadap, and Ravi Ramamoorthi. Deep image-based relighting from optimal sparse samples. *ACM Transactions on Graphics (ToG)*, 37(4):1–13, 2018. 2
- [75] Alex Yu, Ruilong Li, Matthew Tancik, Hao Li, Ren Ng, and Angjoo Kanazawa. Plenotrees for real-time rendering

- of neural radiance fields. In *Proceedings of the IEEE/CVF international conference on computer vision*, pages 5752–5761, 2021. 3
- [76] Ye Yu and William AP Smith. Inverserendernet: Learning single image inverse rendering. In *Proceedings of the IEEE/CVF Conference on Computer Vision and Pattern Recognition*, pages 3155–3164, 2019. 2
- [77] Zehao Yu, Torsten Sattler, and Andreas Geiger. Gaussian opacity fields: Efficient adaptive surface reconstruction in unbounded scenes. *ACM Transactions on Graphics (ToG)*, 43(6):1–13, 2024. 3, 4, 5, 6, 7, 8
- [78] Yu-Jie Yuan, Yang-Tian Sun, Yu-Kun Lai, Yuewen Ma, Rongfei Jia, and Lin Gao. Nerf-editing: geometry editing of neural radiance fields. In *Proceedings of the IEEE/CVF conference on computer vision and pattern recognition*, pages 18353–18364, 2022. 3
- [79] Chong Zeng, Yue Dong, Pieter Peers, Youkang Kong, Hongzhi Wu, and Xin Tong. Dilightnet: Fine-grained lighting control for diffusion-based image generation. In *ACM SIGGRAPH 2024 Conference Papers*, pages 1–12, 2024. 3
- [80] Zheng Zeng, Valentin Deschaintre, Iliyan Georgiev, Yannick Hold-Geoffroy, Yiwei Hu, Fujun Luan, Ling-Qi Yan, and Miloš Hašan. Rgb \leftrightarrow x: Image decomposition and synthesis using material- and lighting-aware diffusion models. In *Special Interest Group on Computer Graphics and Interactive Techniques Conference Conference Papers*, page 1–11. ACM, 2024. 3
- [81] Lvmin Zhang, Anyi Rao, and Maneesh Agrawala. Scaling in-the-wild training for diffusion-based illumination harmonization and editing by imposing consistent light transport. In *The Thirteenth International Conference on Learning Representations*, 2025. 2, 3, 5, 6, 7, 8
- [82] Xiuming Zhang, Sean Fanello, Yun-Ta Tsai, Tiancheng Sun, Tianfan Xue, Rohit Pandey, Sergio Orts-Escolano, Philip Davidson, Christoph Rhemann, Paul Debevec, et al. Neural light transport for relighting and view synthesis. *ACM Transactions on Graphics (TOG)*, 40(1):1–17, 2021. 2
- [83] Xiuming Zhang, Pratul P Srinivasan, Boyang Deng, Paul Debevec, William T Freeman, and Jonathan T Barron. Nerfactor: Neural factorization of shape and reflectance under an unknown illumination. *ACM Transactions on Graphics (ToG)*, 40(6):1–18, 2021. 2, 3
- [84] Qi Zhao, Ping Tan, Qiang Dai, Li Shen, Enhua Wu, and Stephen Lin. A closed-form solution to retinex with non-local texture constraints. *IEEE transactions on pattern analysis and machine intelligence*, 34(7):1437–1444, 2012. 2
- [85] Domenic Zingsheim, Markus Plack, Hannah Dröge, Janelle Pfeifer, Patrick Stotko, Matthias Hullin, and Reinhard Klein. Riftcast: A template-free end-to-end multi-view live telepresence framework and benchmark. In *Proceedings of the 2025 ACM International Conference on Multimedia (ACM MM 2025)*, number 6629, 2025. 5